

Processing and properties of Y-TZP/ Al_2O_3 composites

D. D. UPADHYAYA, P. Y. DALVI, G. K. DEY

Metallurgy Division, Bhabha Atomic Research Centre, Bombay 400 085, India

The processing and property measurement of Y-TZP/ Al_2O_3 ceramic–ceramic composites was investigated. The wet chemical synthesis route was adopted for the preparation of 3Y-TZP matrix dispersed with Al_2O_3 in three different volume fractions. Characterization of the resultant powders was carried out and their densification behaviour was studied by sintering in air in the temperature range 1200–1600 °C. The role of alumina as grain-growth inhibitor for Y-TZP, and the mechanical response of these ultrafine-grain ceramic composites in terms of K_{Ic} characteristics, have been discussed.

1. Introduction

There has been much interest in a new ZrO_2 -based transformation toughened ceramic, termed polycrystalline tetragonal zirconia (TZP) materials. Among these, the alloy systems containing Y_2O_3 , CeO_2 and their mixed variants, have been studied quite extensively over the last several years. These ceramics possess an exceptionally high strength and toughness and have a characteristic ultrafine-grain microstructure. However, problems exist concerning the optimization of fabrication variables due to the transformational instability limit of grain size ($\sim 1 \mu\text{m}$) and about the ubiquitous nature of the intergranular glassy phase.

Considerable microstructural modifications and control have been achieved using powders produced by the wet-chemistry processing route and adopting the densification enhancement techniques of hot pressing and HIPing or by the incorporation of some system-specific dopants [1–4]. For example, a small concentration (0.3 mol %) of transition metal oxides present in the grain-boundary region of Y-TZP, brings down the sintering temperature by about 100 °C and improves the mechanical and thermal properties of the ceramics significantly. The particulate dispersion mode of grain refinement also seems to give a better control on the properties of TZP ceramics. In the system t- $\text{ZrO}_2/\text{Al}_2\text{O}_3$, the components have a limited mutual solubility and thus possess an effective grain-growth inhibition potential for each other [5–7]. Another remarkable feature of Al_2O_3 dispersed Y-TZP ceramics is the gettering effect, i.e. the elimination of impurities (mainly silica) by their reaction with alumina. As a result, the ceramics, when used in solid electrolyte function, exhibit an enhanced electrical conductivity (despite the addition of an insulating phase) [8, 9]. Recent interest has centred on the demonstration of tensile ductility at higher temperatures (≥ 1200 °C) in these composites, due to the fine-grain and coarsening-resistant microstructures [10–12]. The present work mainly deals

with the processing and mechanical property response of 3Y-TZP ceramics containing three different concentrations of Al_2O_3 .

2. Experimental procedure

The wet chemical method of co-precipitation was applied to produce fine powders. Precursor powders of three compositions, 10, 15 and 20 vol % Al_2O_3 , in zirconia stabilized with 3 mol % Y_2O_3 , were selected. The starting materials were high-purity salts of $\text{ZrOCl}_2 \cdot 8\text{H}_2\text{O}$, $\text{Y}(\text{NO}_3)_3 \cdot 5\text{H}_2\text{O}$ and $\text{Al}(\text{NO}_3)_3 \cdot 9\text{H}_2\text{O}$, respectively. The required quantity of each salt was weighed and stock solutions with a cation concentration of 0.5 M were prepared by dissolving in distilled water. Mixed solution was then added drop wise to a vigorously stirred 6M NH_4OH solution which produced a white, gelatinous precipitate. To ensure complete reaction, an excess of ammonia was used and the pH was maintained above 10 during precipitation.

The resulting gels were filtered and thoroughly washed with distilled water and finally dehydrated with ethyl alcohol and dried at 110 °C overnight. The dried mass was crushed and calcined at 600 °C for 3 h in an air atmosphere. The resulting product was ball-milled for 8 h using TZP grinding medium. X-ray diffraction analysis was performed on the precursor calcined powders. Compacts for sintering were prepared by cold pressing at 84 MPa in a hardened steel die using 1 wt % stearic acid in acetone as a die lubricant. Samples were fired in air between 1200 and 1600 °C for 2 h.

The bulk density of sintered samples was estimated by the water displacement method. Phase identification of as-fired and polished surfaces of the specimens was carried out by the polymorph method of Garvie and Nicholson [13]. It used the intensity ratio of monoclinic (1 1 1) and (1 1 $\bar{1}$) to tetragonal (1 1 1) reflections for estimation of the relative fraction of m- ZrO_2 phase. Microhardness was measured by Vickers indentation method using loads from 100–300 N. Frac-

ture toughness, K_{Ic} , was estimated using the procedure given by Anstis *et al.* [14]. For transmission electron microscopy studies the sintered samples were diamond sliced to about 250 μm thin sections and 3 mm diameter discs were prepared by ultrasonic cutter and were further mechanically thinned using a disc-grinder followed by dimple grinding using diamond paste. The final thinning was done by argon ion-milling to electron transparency.

3. Results and discussion

The transformation toughening phenomenon in ZrO_2 has been effectively harnessed in the form of ZTA ceramics [15, 16]. These dual-phase ceramics generally contain 10%–30% zirconia fine dispersions in an alumina matrix. This results in considerable improvement in strength, toughness and other physical properties over the single-phase alumina ceramics. A similar approach was also used for the zirconia-rich compositions, particularly the Y-TZP and (Ce, Y)-TZP alloys, in which the alumina dispersion was found to play the role of a grain refiner, to improve elastic modulus and to suppress the $t \rightarrow m$ phase transformation during low-temperature ageing [10, 17]. The characteristic fine and isometric grain structure and the absence of transformation toughening above 1100 $^\circ\text{C}$ lowers the creep resistance and thus makes these materials amenable to post-sintering hot-forming processes. The present work deals mainly with the preparation of three precursor powders, their pressureless sintering behaviour and evaluation for fracture toughness parameter.

Fig. 1 shows the X-ray powder diffraction patterns for the matrix material (3Y-TZP) and the composite batch (3Y-TZP/10 vol % Al_2O_3) after calcination at 600 $^\circ\text{C}$. A marked difference in crystallization behaviour is obtained between the two materials synthesized under identical conditions. The weak-intensity, diffuse reflections for the latter suggest a poorly crystalline nature of the composite powder. The inhibition of crystallization reaction can be attributed to the stability of Zr–O–Al bonds and the mutual interaction of the two developing phases. The higher fractal dimension on hydroxide decomposition produces them in the ultrafine form [18]. Fig. 2 presents the densification behaviour of these powders containing different concentrations of alumina. The important features are (i) an inverse dependence of the rate of the densification on the alumina content, and (ii) a reasonably linear rise in density with increasing sintering temperature up to an optimum of about 95% relative density, for all three compositions studied. An appreciable expansion of densification regime over the whole sintering range for composite powders is a remarkable feature compared to pure TZP powders. For the latter, densification rapidly accelerates towards the final density in a narrow temperature range of 1300 \pm 50 $^\circ\text{C}$, thus requiring a delicate balance of sintering parameters.

The retardation in densification rate can readily be ascribed to the reduced grain-boundary mobility of the zirconia matrix with increasing ratio of alumina

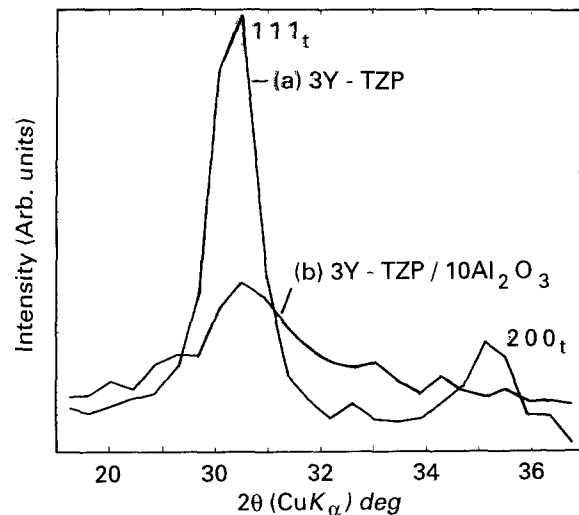


Figure 1 X-ray diffraction patterns of 3Y-TZP, (a) without alumina, and (b) with 10 vol % alumina.

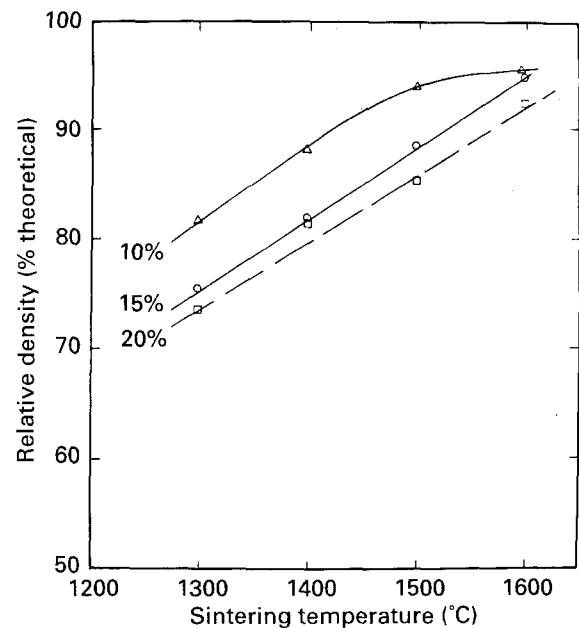


Figure 2 Plot of relative density versus sintering temperature for Al_2O_3 -dispersed TZP composites.

reinforcement, because long-range interdiffusion is limited owing to an increase in the diffusion path lengths relative to single-phase geometry [19–20]. An identical behaviour was also observed for zirconia-dispersed alumina ceramics, showing an increase in grain-growth restraint with higher volume fraction of dispersoid. Another phenomenon operating in these biphasic systems (particularly for the low volume fraction) is that the isolated second-phase particles become coarsened by coalescence as they are dragged by moving grain boundaries [16, 17]. These effects thus contribute to the grain stabilization of both the constituent phases.

For the present composite system its manifestation could be seen in terms of the variation in metastable t -phase retention capability of the sintered products. The extent of transformation instability was found to be a function of sintering temperature and Al_2O_3 content. This has been represented qualitatively in

Fig. 3 by the XRD profiles for samples containing 10% and 15% Al_2O_3 which were sintered at 1500°C for 2 h. Under these sintering conditions, as shown for (a), a significant fraction of TZP matrix starts transforming to the m-phase (leading to micro-cracking and consequential strength property degradation). However, the spontaneous transformation could successfully be prevented, as found in case (b), by incorporating a higher concentration (15%) of alumina. Thus a suitable control of the above two critical processing parameters facilitates tailoring of a composite displaying optimum performance.

Mechanical behaviour of sintered composites was examined by estimating the microhardness and fracture toughness, K_{Ic} , values. Fig. 4 shows the compositional dependence of K_{Ic} for composites prepared under three different sintering conditions. A marked

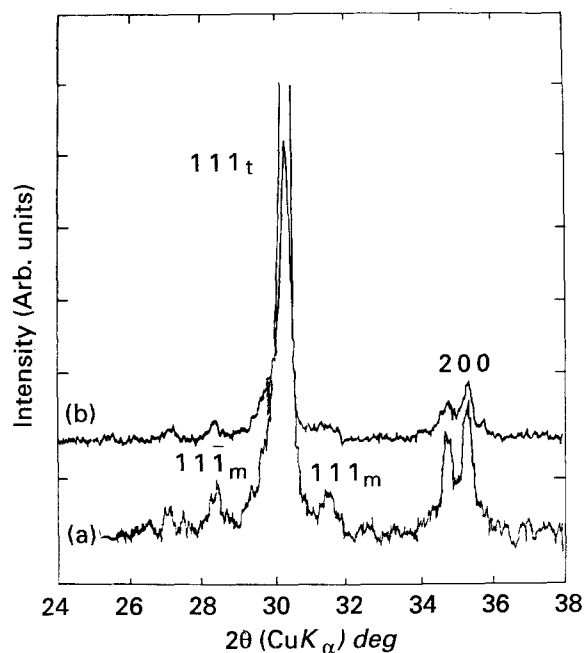


Figure 3 X-ray diffraction patterns of 3Y-TZP/ Al_2O_3 composites containing (a) 10 vol% and (b) 15 vol% alumina, sintered at 1500°C for 2 h.

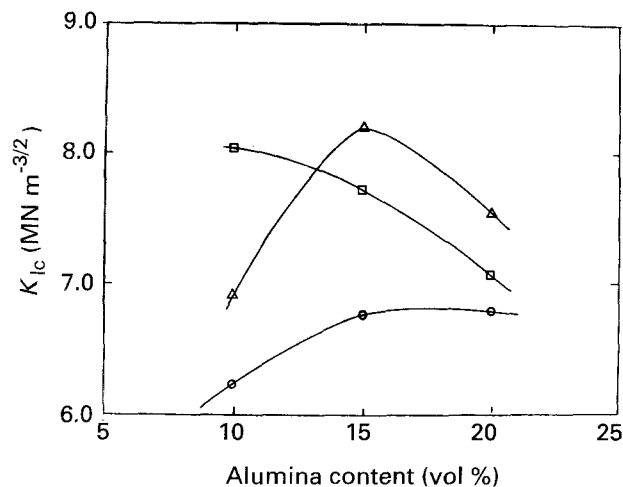


Figure 4 Fracture toughness, K_{Ic} , of 3Y-TZP/ Al_2O_3 composites as a function of alumina content, sintered for 2 h at (○) 1400°C , (△) 1500°C and (□) 1600°C .

difference in K_{Ic} dependence on sintering temperatures was observed. At 1400°C , a gradual rising trend was observed reaching a constant value of about $6.7 \text{ MN m}^{-3/2}$ for higher ($> 15\%$) Al_2O_3 content. On sintering at 1500°C , the highest value of $K_{Ic} = 8.2 \text{ MN m}^{-3/2}$ was attained for compacts containing an intermediate volume fraction (15%) of dispersed phase, and then falling sharply beyond this value. When sintered at 1600°C it shows a steadily decreasing trend with increasing alumina content over the composition range studied in the present work.

The observed K_{Ic} pattern in Fig. 4 can readily be understood in terms of the cumulative effect of two variables, i.e. the bulk density and the t-phase content of the composites. A low fracture toughness value for the less-dense state of the ceramic is a general feature, but the relative contribution of the transformation toughening phenomenon has resulted in the difference in K_{Ic} . The latter again seems to depend on the alumina content and the sintering temperature employed, e.g. for 15% Al_2O_3 the optimum fracture toughness is obtained by sintering at 1500°C . At higher temperature sintering, in general the property deteriorates due to the $t \rightarrow m$ phase transformation which is accompanied by the formation of micro-cracks. Thus K_{Ic} results are the product of equilibrium conditions in respect of grain-size restraint of Y-TZP matrix (by alumina addition) and the counteracting parameter of transformational instability induced by high-temperature sintering.

The representative micrograph in Fig. 5a shows the microstructural evolution in these composites. Reasonably uniform and fine grains, with a mean size of approximately 500 nm, were obtained both for the matrix and dispersed phases. Some clustering of discrete alumina particles was generated during sintering. This coalescence effect can be attributed to the dragging of Al_2O_3 particles by migrating ZrO_2 grain boundaries and their eventual segregation at suitable low-energy sites [16]. The matrix grains are completely pore-free and show the characteristic ferroelastic twin contrast of t- ZrO_2 . Fine pores ($< 50 \text{ nm}$) were, however, trapped preferentially within the alumina grains. This residual porosity is evidently due to the microporous textures in the low-temperature modifications of alumina which, again, is dependent on the length of the OH^- bonds in hydroxides.

The other interesting feature, particularly for compositions containing a lower volume fraction of second phase, was with respect to the geometry of non-interacting dispersoid. As shown in Fig. 5, such particles, as a result of high grain co-ordination number, tend to acquire a concave interface. This configuration prevents the Ostwald ripening process of diffusion and thus provides a self-refining mechanism to generate a mutually coarsening-resistant micro-duplex structure.

The single-phase Y-TZP ceramics usually possess a bimodal grain distribution and a pronounced surface grain-coarsening tendency on high-temperature annealing [21]. This surface microstructural change was explained to be due to a diffusional transformation (tetragonal to cubic phase) of ZrO_2 induced by surface

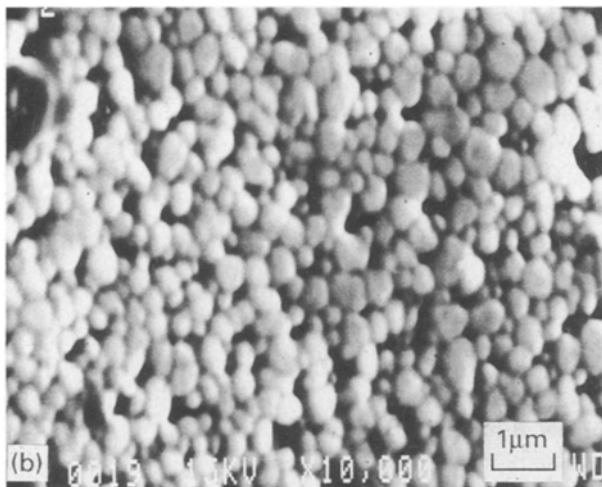
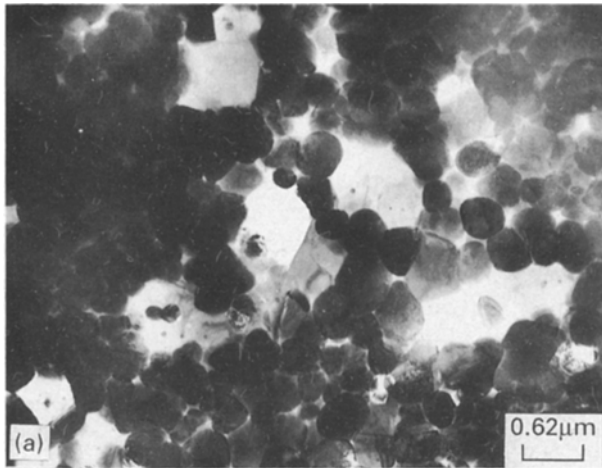


Figure 5 (a) Transmission electron micrograph of 3Y-TZP/10 vol % Al_2O_3 composite sintered at 1400°C for 2 h. The bright phase containing pores is Al_2O_3 and the dark phase is t-ZrO₂. (b) Scanning electron micrograph of surface microstructure of 3Y-TZP/10 vol % Al_2O_3 sample after refiring at 1400°C for 2 h. The light phase is 3Y-TZP matrix and the dark phase is Al_2O_3 dispersoid.

segregation of Y_2O_3 in the presence of grain-boundary siliceous liquid phase. Alumina reinforcement of Y-TZP was observed to suppress effectively the anomalous growth behaviour. As shown in Fig. 5b for 3Y-TZP/10 vol % Al_2O_3 composites, a fine-grained and a reasonably uniform grain size was maintained after reheating the polished samples at 1400°C for 2 h. The alumina dispersion in Y-TZP is beneficial in generating an ultrafine-grained microstructure which is also stable against coarsening at elevated temperatures.

Conclusions

1. Compared to pure TZP, the 3Y-TZP/ Al_2O_3 precursor was found to inhibit significantly the crystallization process of the individual phases. The effect increases with increasing proportion of dispersed phase.

2. Fracture toughness for the composites, however, attains a higher value but shows a critical dependence on the amount of alumina and the sintering temperature employed.

3. Electron microscopy results support the interpretations concerning the interphase interactions producing the favourable grain growth inhibition effect. The processing conditions employed were found to be satisfactory for achieving a homogeneous particulate reinforcement in the ZrO_2 -based ceramic-matrix composites.

Acknowledgements

The authors thank Dr S. Banerjee, Head, Metallurgy Division, for his keen interest and encouragement, and also Dr S. K. Roy, Dr R. Bhat and Shri O. K. Mehra, for helpful discussions.

References

1. K. KEIZER, M. J. VERKAR and A. J. BURGGRAB, *Ceram. Int.* **5** (1970) 145.
2. N. KIMURA, S. ABE, Y. MAYASHI, J. MORISHITA and H. OKAMURA, in "Ceramic Powder Processing Science", edited by M. Hausener, G. L. Mersing and S. Hirano (Dutsche Kiramische Gassellschaft, Koln, 1988) p. 765.
3. T. MASAKI and K. SINJO, *Ceram. Int.* **13** (1987) 109.
4. S. L. HWANG and I. W. CHEN, *J. Am. Ceram. Soc.* **73** (1990) 3269.
5. K. TSUKUMA, K. UEDA, K. MATSUSHITA and S. SHIMADA, *ibid.* **68** (1985) C-56.
6. M. RUHLE and A. G. EVANS, *Prog. Mater. Sci.* **33** (1989) 85.
7. S. M. SIM, A. MORRONE and D. E. CLARK, *Ceram. Eng. Sci. Prog.* **11** (1990) 1712.
8. S. RAJENDRAN, J. DRENNAN and S. P. S. BADWAL, *J. Mater. Sci.* **6** (1987) 1431.
9. J. DRENNAN and E. P. BUTLER, *Sci. Ceram.* **12** (1984) 267.
10. T. G. NIEH, C. M. McNALLY and J. WADSWORTH, *Scripta Metall.* **23** (1989) 457.
11. F. WAKAI, Y. KODAMA and T. NAGANO, *Jpn. J. Appl. Phys. Ser. 2* (1989) 57.
12. F. WAKAI and H. KATO, in "Ultrastructure Processing of Advanced Ceramics", edited by J. D. Mackenzie and D. R. Ulrich (Wiley, New York, 1989) Ch. 50.
13. R. C. GARVIE and P. S. NICHOLSON, *J. Am. Ceram. Soc.* **55** (1972) 303.
14. G. R. ANSTIS, P. CHANTIKUL, B. R. LAWN and D. B. MARSHALL, *ibid.* **64** (1981) 533.
15. N. CLAUSSEN and M. RUHLE, in "Advances in Ceramics", Vol. 3, edited by A. H. Heuer and L. W. Hobbs (American Ceramic Society, Columbus, OH, 1981) p. 137.
16. P. Y. DALVI and D. D. UPADHYAYA, *Trans. Ind. Ceram. Soc.* **49** (1990) 21.
17. B. KIBBEL and A. H. HEUER, *J. Am. Ceram. Soc.* **69** (1986) 231.
18. J. WANG and R. RAJ, *ibid.* **74** (1991) C-1707.
19. T. S. YEH and M. D. SOCKS, *ibid.* **71** (1988) 841.
20. F. F. LANGE and M. M. HIRLINGER, *ibid.* **70** (1985) 827.
21. R. CHAIM, D. G. BRANDON and A. H. HEUER, *Acta Metall.* **34** (1986) 1933.

Received 8 July 1992

and accepted 30 April 1993